

Cite this: *RSC Advances*, 2012, 2, 2284–2288

www.rsc.org/advances

COMMUNICATION

Elastic magnetic sensor with isotropic sensitivity for in-flow detection of magnetic objects

Michael Melzer,^a Daniil Karnausenko,^{ab} Denys Makarov,^{*a} Larysa Baraban,^a Alfredo Calvimontes,^c Ingolf Mönch,^a Rainer Kaltofen,^a Yongfeng Mei^d and Oliver G. Schmidt^{ab}

Received 10th November 2011, Accepted 9th January 2012

DOI: 10.1039/c2ra01062c

We present a conceptually new approach for the detection of magnetic objects flowing through a fluidic channel. We produce an elastic and stretchable magnetic sensor and wrap it around capillary tubing. Thus, the stray fields induced by the flowing magnetic objects can be detected virtually in all directions (isotropic sensitivity), which is unique for elastic sensors when compared to their rigid planar counterparts.

Magnetic particles are widely used for diagnostic or therapeutic purposes in biology and medicine,^{1,2} implying the necessity of implementation of magnetic field sensors in complex biomedical systems. In this respect, magnetic field sensors relying on magnetoresistive effects and especially on the giant magnetoresistive (GMR) effect^{3,4} represent an efficient solution for the use in fluidic biodetection platforms due to their high sensitivity. Planar^{5,6} as well as rolled-up⁷ magnetic sensors are already incorporated in *microfluidic* channels enabling detection of magnetic particles. Fabrication of these magnetic sensors requires intensive lithography processing and is therefore expensive and time consuming. In contrast, for the dynamically developing *millifluidic* approach,^{8–10} which implies the use of the millimetre size objects, a sensor can be of a larger size and its design can be substantially simplified. In this case, cost effective solutions for a magnetic sensor with an attractive possibility to be easily integrated into a system and to be reused many times are of great advantage.

Here, we propose a new concept based on stretchable magnetoelectronics,¹¹ which can attain the above mentioned requirements in an elegant way. Stretchable (magneto)electronics^{11–14} combine the advantages of being flexible with the speed and performance of conventional semiconductor-based electronics.^{15,16} We show that a stretchable GMR sensor can be efficiently implemented in a fluidic system for detection of the stray fields of magnetic particles in a

suspension.¹⁷ Indeed, given that the elastic sensor can be wrapped tightly around the fluidic channel, as shown conceptually in Fig. 1(a), isotropic sensitivity can be expected, due to the imposed cylindrical symmetry. This is a unique feature of elastic magnetic sensors compared to their rigid planar counterparts, detecting only a component of the magnetic stray field of the object, parallel to the sensor's plane, thus limiting the possibility for efficient and quantitative detection of small magnetic fields. In addition, cylindrical symmetry of the wrapped sensors makes the detected signal less dependent on the position of a magnetic object inside the tubing, since the sensing element covers its entire circumference. Therefore, we can diminish the need of applying an external magnetic bias field to align the magnetic moment of the particles with the direction of maximum sensitivity of a conventional planar sensor. Finally, in combination with magnetic particles as biomarkers,¹⁸ this elastic magnetic sensor can be considered as a new generation of biosensors for cells or even biomolecules^{19,20} evading many difficulties of traditional optical detection methods like low speed, excitation, bulky and expensive equipment, biomolecular amplification and the need for transparent packaging.

Detection of magnetic particles in fluidic flow requires high sensitivity of the sensor to magnetic fields in the range of 1 mT and below.^{5,7,20–23} Maximizing the sensitivity of a magnetic sensor on elastomeric membrane is therefore a crucial task. For this purpose, we fabricated different GMR multilayer systems, including Co/Cu and Py/Cu stacks (Py = Ni₈₁Fe₁₉), on a free-standing rubber membrane. In all cases the GMR systems reveal a similar GMR performance on the poly(dimethylsiloxane) (PDMS) membrane and on rigid SiO_x wafers. We demonstrate that the sensitivity of the Py(1.5 nm)/[Py(1.5 nm)/Cu(2.3 nm)]₃₀ multilayers coupled in the 2nd antiferromagnetic (AF) maximum and grown onto 40 μm thick elastic PDMS membrane is a remarkably high 106 T⁻¹, with a maximum at a field of 0.8 mT.

Details on the fabrication of elastic magnetic sensors (Co/Cu and Py/Cu multilayers coupled in the 1st and 2nd AF maximum) and comparison of their magnetoelectric properties are given in the Experimental section. Due to its high sensitivity at small magnetic fields, the optimized [Py/Cu]₃₀ GMR sensor coupled in the 2nd AF maximum was chosen for millifluidic experiments on the in-flow detection of magnetic FeNdB particles.

The GMR curves measured at room temperature on the [Py/Cu]₃₀ samples prepared on different substrates are shown in Fig. 2(a). The

^aInstitute for Integrative Nanosciences, IFW Dresden, Helmholtzstr, 20, 01069, Dresden, Germany. E-mail: m.melzer@ifw-dresden.de; d.karnausenko@ifw-dresden.de; d.makarov@ifw-dresden.de; l.baraban@ifw-dresden.de; i.moench@ifw-dresden.de; r.kaltofen@ifw-dresden.de; o.schmidt@ifw-dresden.de

^bMaterial Systems for Nanoelectronics, Reichenhainer Strasse, 70, 09107, Chemnitz, Germany

^cLeibniz Institute of Polymer Research Dresden, 01069, Dresden, Germany. E-mail: calvimontes@ipfdd.de

^dDepartment of Materials Science, Fudan University, Shanghai, 200433, People's Republic of China. E-mail: yfm@fudan.edu.cn

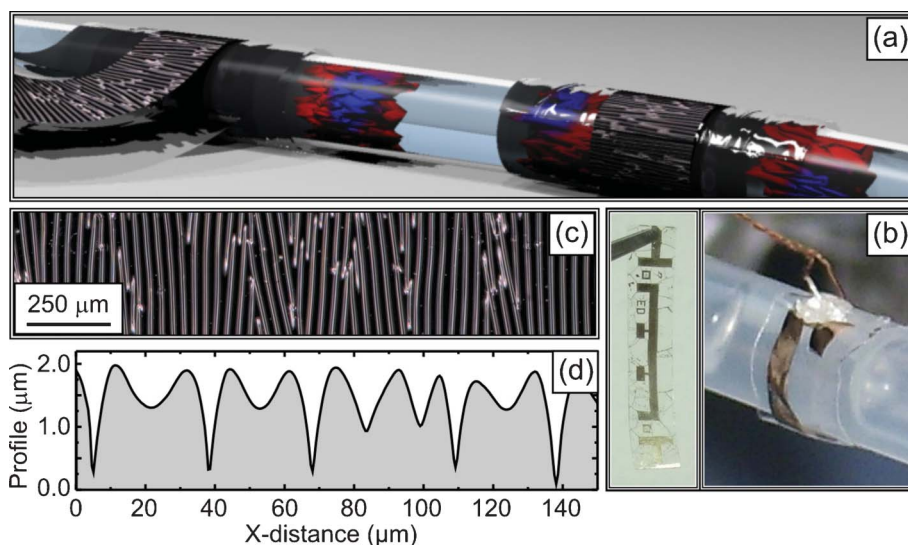


Fig. 1 (a) Sketch demonstrating the application of stretchable magnetic sensors for in-flow detection of magnetic objects in fluids: the elastic sensor can be tightly wrapped around a fluidic channel allowing for an enhanced and isotropic sensitivity. (b) Elastic [Py/Cu]₃₀ GMR sensor: (left panel) as-prepared and (right panel) wrapped around the circumference of a Teflon tube. (c) Optical microscopy image of a wrinkled [Py/Cu]₃₀ magnetic sensor prepared on an elastic PDMS membrane. (d) Line scan taken of the confocal microscopy image (Experimental section) revealing the topography of the wrinkled GMR multilayer stack.

GMR ratio is defined as the magnetic field dependent change of the sample's resistance, $R(H_{\text{ext}})$, normalized to the value of resistance when the sample is magnetically saturated, R_{sat} : $\text{GMR}(H_{\text{ext}}) = [R(H_{\text{ext}}) - R_{\text{sat}}]/R_{\text{sat}}$.²⁴ The GMR curves obtained from the samples prepared on a rigid SiOx wafer without (open square symbols) and with PDMS coating (open circle symbols) are similar. Furthermore, the GMR signal does not change after the PDMS is peeled off the SiOx wafer (Fig. 2(a)), compare curves with open and closed circle symbols). Fig. 2(a) also includes the magnetic field dependent sensitivity of the GMR sensors fabricated on the free-standing rubber membrane (filled triangles). Here, the sensitivity of the sensor element is defined as the first derivative of the sample's resistance over the magnetic field divided by the resistance value: $S(H_{\text{ext}}) = [dR(H_{\text{ext}})/dH_{\text{ext}}]/R(H_{\text{ext}})$.²⁴ The obtained GMR curve is narrow with a very low saturation field and a considerable resistance change of more than 13%. The sensitivity of this sensor reaches a remarkable value of 106 T^{-1} , which is almost 30 times larger than for the [Co/Cu]₅₀ coupled in the 1st AF maximum (see Experimental section). Also, the maximum of sensitivity is at very low fields of 0.8 mT. In order to also obtain isotropic sensitivity, the sensor has to be tightly bent according to the circumference of the millifluidic tubing (right side of Fig. 1(b)); and thus it has to withstand strong mechanical deformations. Therefore, the stability of the sensor against tensile strains is investigated in more detail.

The free-standing PDMS rubber membranes with the photolithographically patterned [Py/Cu]₃₀ GMR multilayers on top (left side of Fig. 1(b)) were mounted onto a motorized stretching device, which fits between the poles of an electromagnet for magneto-electric characterizations. The electrical resistance of the sample upon stretching was measured using a four-probe method. The measurement routine includes applying an external uniaxial stress to the sample and, for each strain value, recording a GMR curve. It was carefully checked that the strain applied to the rubber is completely transferred to the wrinkled GMR multilayer stack.¹¹ Fig. 2(b) shows the strain dependent sample resistance (black squares) and GMR magnitude (red circles) of the [Py/Cu]₃₀ sensor during stretching. The

curves show that the resistance remains fairly constant for tensile strains below 1% and gradually increases for higher strain values. However, the electrical contact is maintained for strains up to 2%. The remarkable stretchability of the thin metal layer on top of the rubber is due to a thermally induced wrinkling effect²⁵ which protects the film from cracking and breaking by smoothing out the buckles during elongation of the rubber substrate.²⁶ Optical microscope images as well as a line scan from a confocal microscope image (Experimental section) of the wrinkled GMR film are shown in Fig. 1(b, c). The wrinkling phenomenon of the GMR stacks on free-standing PDMS membranes was previously discussed in detail.¹¹ The most striking aspect of the stretching experiment is that although the absolute resistance of the sensor element is increasing by a factor of about 8, the GMR ratio (*e.g.* the relative resistance change due to the external magnetic field) remains at a constant level (Fig. 2(b), red circles). The GMR curves obtained for each applied strain value match accurately (inset in Fig. 2(b)). This suggests that even if the metallic film is partly damaged by the imposed tensile strain, the GMR effect is still present without major deterioration and the sample acts as a magnetic sensor element.

To demonstrate the capabilities of the stretchable [Py/Cu]₃₀ GMR sensor with optimized sensitivity for in-flow detection of magnetic particles, we designed a millifluidic circuit using a Teflon tube (inner diameter: 1.5 mm; outer diameter: 3.2 mm). Due to the elasticity of the presented sensor elements it is possible to wrap the GMR film on the rubber membrane around the entire outer circumference of the millifluidic channel (Fig. 3(a)). The fluidic circuit allows the flow of magnetic particles inside the tube towards the sensing element. The sensor was contacted for a two-probe measurement of the electrical resistance with thin copper wires (0.1 mm) using conductive silver paste and connected to the data acquisition hardware (Experimental section). The experiment was performed using commercially available FeNdB magnetic particles (FOB Shanghai, Ref. Nr. QJK-ES) dispersed in a mineral oil (Sigma Aldrich, M5904). 2%_{v/v} of sorbitane monooleate (Sigma Aldrich, S6760) was added to reduce the wetting of the dispersion on the tube walls. Magnetic

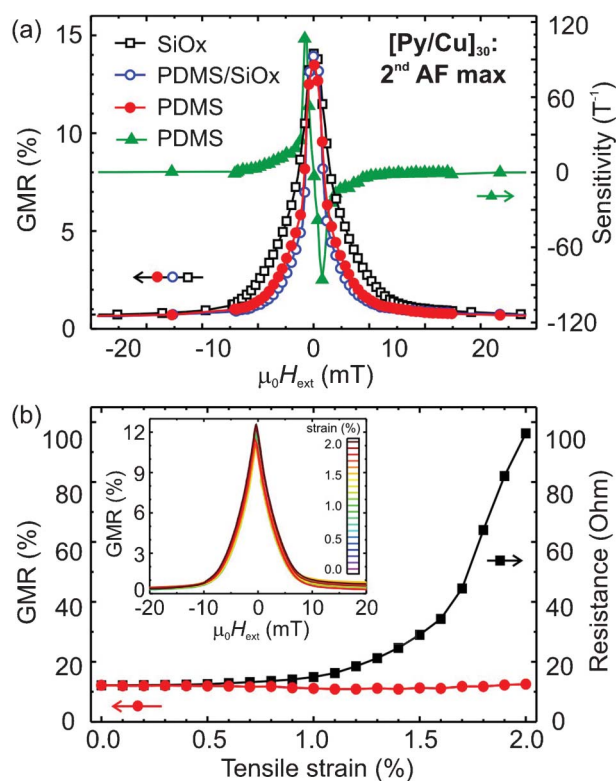


Fig. 2 (a) GMR curves of the $[\text{Py}/\text{Cu}]_{30}$ GMR multilayers coupled in the 2nd AF maximum. The GMR sensors are fabricated on different substrates: (open squares) rigid SiOx wafer, (open circles) PDMS coated SiOx wafer, and (filled circles) free-standing PDMS membrane. Field dependent sensitivity of the GMR sensors on free-standing PDMS membranes is also shown (filled triangles). Inset in panel (a) is the magnified view of the GMR and sensitivity curves. (b) GMR magnitude (circles) and sample resistance (squares) in dependence of the imposed tensile strain for the $[\text{Py}/\text{Cu}]_{30}$ multilayer stack. Inset in panel (b) shows the series of GMR curves measured for different strain values. The strain values are color coded. The data demonstrates that GMR curves match well, up to the strain value of 2%.

characterization of the FeNdB particles is provided in the Experimental section. When placed in liquid, the magnetic particles quickly aggregate, forming macroscopic clusters with sizes of about 1 mm. These clusters were pumped into the fluidic channel. In order to separate neighbouring clusters for detection, water droplets, coloured by red ink, were injected into the channel as spacers (Fig. 3(b)). As the magnetic particles appear in close vicinity of the GMR detector the total resistance of the sensor element decreases, resulting in an easily detectable voltage change of the sensor's output. Several consecutive in-flow detection events are demonstrated in Fig. 3(c) by monitoring the time evolution of the sensor's output. The signal to noise ratio is about 13 dB, which allows detecting reliably the magnetic objects of interest and suggests that even smaller particles can be detected.

In conclusion, we demonstrated a new concept for in-flow detection of magnetic particles in millifluidics using *elastic magnetic sensors* relying on the giant magnetoresistive (GMR) effect. Due to their stretchability, GMR sensors can be wrapped tightly around a fluidic channel. This strategy offers the following advantages: (i) sensing of the magnetic stray fields in virtually all directions (isotropic sensitivity), which is unique compared to the rigid planar

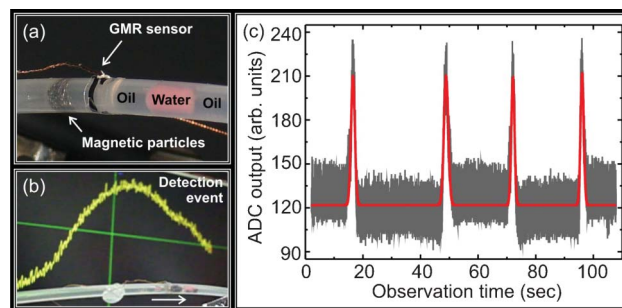


Fig. 3 Detection of magnetic particles in a fluidic channel: (a) optimized $[\text{Py}/\text{Cu}]_{30}$ elastic GMR sensor wrapped around the circumference of a Teflon tube. Agglomerate of FeNdB particles suspended in oil and separated by colored water droplets inside the tubing is shown. The magnetic particles are approaching the GMR sensor. (b) Signal of the elastic GMR sensor on a screen (background) as the magnetic cluster is passing the sensor (foreground). (c) Several consecutive detection events of particles passing the elastic GMR sensor.

counterparts; (ii) simplicity of the sensor integration into a fluidic circuit; (iii) possibility of being reused. As magnetic stray fields to be detected in fluidics are small, a strong emphasis was on the enhancement of the sensitivity of the sensor on elastic membranes to small magnetic fields. For this purpose, we fabricated different GMR multilayer systems, including Co/Cu and Py/Cu stacks (Py = $\text{Ni}_{81}\text{Fe}_{19}$) coupled in the 1st or 2nd AF maximum. Even when prepared on elastic, 40 μm thick, free-standing rubber membranes, Py/Cu multilayers coupled in the 2nd AF maximum reveal a remarkable sensitivity of 106 T^{-1} (magnetic field: 0.8 mT); this value is almost 30 times larger than for the Co/Cu stack coupled in the 1st AF maximum. These Py/Cu GMR sensors with optimized sensitivity are fully operational under elastic tensile deformations due to a thermally induced wrinkling of the multilayer stack. We successfully demonstrate on a proof-of-concept level the performance of this elastic sensor wrapped around a fluidic channel for in-flow detection of magnetic FeNdB particles. Our approach potentially opens an exciting possibility for stretchable magnetoelectronics to be applied in the field of biology and chemistry.

Experimental

Magnetic sensors on a free-standing PDMS membrane

In order to fabricate GMR layer stacks on a free-standing rubber membrane, PDMS (Sylgard 184) was first spin-coated onto SiOx wafers. An antistick photoresist layer was introduced to assist peeling the PDMS film from the rigid support. The PDMS precursor blend was cured in an oven at $120 \text{ }^\circ\text{C}$ for 30 min under continuous nitrogen flow, resulting in a rubber film thickness of 40 μm . In addition, photolithographic patterning on the PDMS surface before deposition of the metal films was performed to allow for reliable electrical resistance measurements of the GMR films on the rubber substrates. This renders the fabrication process compatible to current micro-electronic structuring procedures. Different GMR multilayer stacks were grown on the elastic PDMS surface using magnetron sputter deposition at room temperature (base pressure: 7.0×10^{-8} mbar; Ar sputter pressure: 7.5×10^{-4} mbar; deposition rate of about $1 \text{ } \text{\AA} \text{ s}^{-1}$). After deposition the PDMS membrane carrying the GMR multilayers are peeled from the SiOx wafer by means of the antistick layer

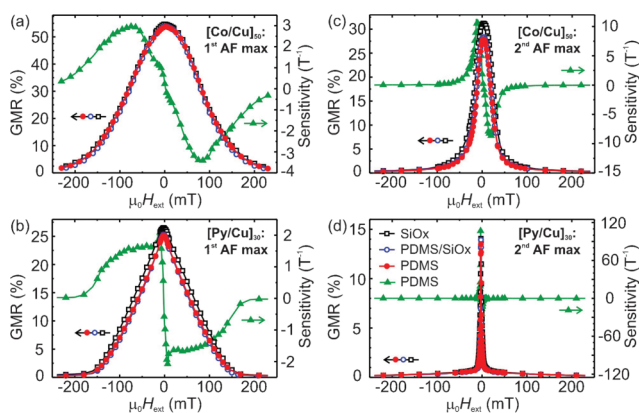


Fig. 4 GMR curves of the four investigated GMR multilayer stacks: (a) $[\text{Co}/\text{Cu}]_{50}^{1\text{st}}$, (b) $[\text{Py}/\text{Cu}]_{30}^{1\text{st}}$, (c) $[\text{Co}/\text{Cu}]_{50}^{2\text{nd}}$, and (d) $[\text{Py}/\text{Cu}]_{30}^{2\text{nd}}$. The GMR sensors are fabricated on different substrates: (open squares) rigid SiOx wafer, (open circles) PDMS coated SiOx wafer, and (filled circles) free-standing PDMS membrane. The field dependent sensitivity of the GMR sensors on free-standing PDMS membranes is also shown (filled triangles).

leading to a free-standing elastic membrane covered with a lithographically patterned GMR sensor element.

Optimization of the sensitivity of magnetic sensors on a free-standing PDMS membrane

Starting from the well known Co/Cu GMR system coupled in the 1st AF maximum ($[\text{Co}/\text{Cu}]_{50}^{1\text{st}}$) with its notorious GMR magnitude, there are two approaches to enhance the sensitivity of the GMR multilayer sensor that are approved for rigid substrates.³ On the one hand, the magnetically softer Permalloy (Py) can be used as the ferromagnetic layers ($[\text{Py}/\text{Cu}]_{30}^{1\text{st}}$). On the other hand, magnetic layers in the multilayer stack can be coupled in the 2nd AF maximum by increasing the thickness of the nonmagnetic spacer layers ($[\text{Co}/\text{Cu}]_{50}^{2\text{nd}}$). Finally, a combination of both approaches is applied by preparing a Py/Cu multilayer coupled in the 2nd AF maximum ($[\text{Py}/\text{Cu}]_{30}^{2\text{nd}}$). This accounts for the four different GMR multilayer systems investigated in the present work. The GMR curves of all these multilayer systems measured at room temperature on rigid and elastic substrates are shown in Fig. 4 together with their field dependent sensitivity on free-standing PDMS.

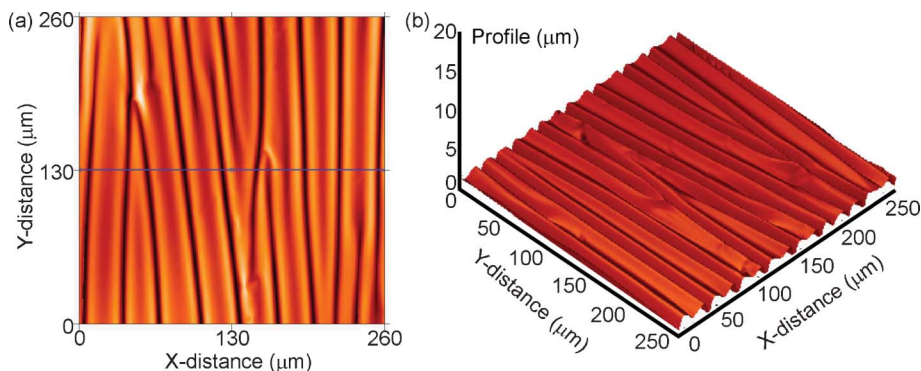


Fig. 5 Thermally induced wrinkling of GMR multilayers with optimized sensitivity ($[\text{Py}/\text{Cu}]_{30}^{2\text{nd}}$ multilayer stack coupled in the 2nd AF maximum) on top of a free-standing rubber membrane. Confocal microscopy image of the sample surface: (a) 2D image and (b) 3D image.

Topography of the wrinkled metal surface on a free-standing PDMS membrane

In order to access the topography of the wrinkled magnetic sensor after peeling the PDMS from the rigid SiOx wafer, a confocal microscopy study was performed (Fig. 5). The line-scan presented in Fig. 1(c) of the manuscript is taken along the blue line indicated in Fig. 5(a).

Furthermore, our experimental setup allows *in situ* measurements of the morphology of a sample (magnetic sensor on a polymer membrane) using optical microscopy during stretching. Analysis of the series of optical images allowed a calibration curve to be built, [applied strain using stretching device] vs. [measured strain on the sample]. The measured dependence is linear with a slope equal to one. Based on this curve, we conclude that the strain applied to the rubber is completely transferred to the GMR multilayer.

In-flow detection of magnetic particles in millifluidics

The GMR sensor with optimized sensitivity ($[\text{Py}/\text{Cu}]_{30}^{2\text{nd}}$ multilayer stack coupled in the 2nd AF maximum) was wrapped around a Teflon tube with an outer diameter of 3.2 mm. No adhesive was used to attach the sensor to the tubing. Electrical connection of the sensor to a home-made single board acquisition device was realized using a twisted pair cable in a two point measurement configuration by gluing copper wires to the sensor utilizing silver paint (ACHESON Silver DAG 1415). The sensor's response to an applied magnetic field was detected by measuring the changes in its resistance. The sensor bias current, produced by a constant current generator circuit implemented directly on the acquisition device, was set to 20 mA. The voltage signal from the sensor was amplified and fitted to the input range of an analog to digital converter (ADC) embedded in a micro controller unit (MCU) C8051F342 of the acquisition device. The acquired data was processed in the MCU and sent to a personal computer (PC) *via* an universal serial bus (USB2.0) interface at a rate of 2000 measured points per second.

Magnetic characterization of the FeNdB particles

A study of the magnetic properties of the purchased FeNdB powder (FOB Shanghai, Ref. Nr. QJK-ES) was carried out at room temperature using vibrating sample magnetometry (VSM). The hysteresis loop shown in Fig. 6 reveals a high value of remanent magnetization of about 0.66 (normalized to the saturation

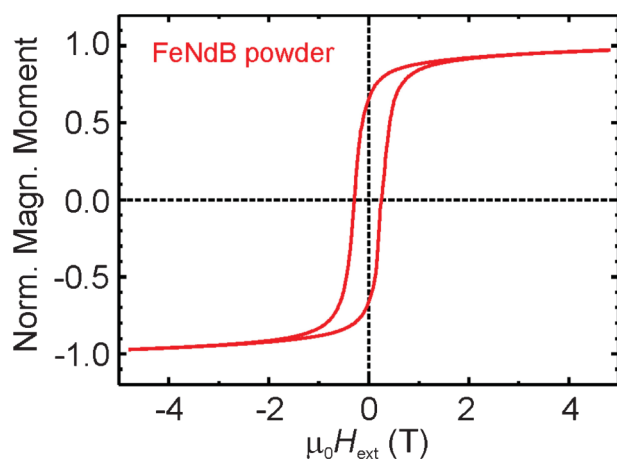


Fig. 6 Magnetic hysteresis loop of FeNdB powder measured at room temperature using VSM.

magnetization), which is crucial for the purpose of our experiment. Composition of the as-purchased magnetic powder is $\text{Fe}_{67}\text{Nd}_{22}\text{B}_{10}$.

Acknowledgements

The authors acknowledge valuable discussions with Dr S. Sanchez. The support in the development of the experimental setups from Dr R. Träger is greatly appreciated. We thank I. Fiering for the assistance in the deposition of the magnetic layers, B. Eichler for the AFM imaging, M. von Papen for support with optical microscopy imaging using Keyence VHX-1000 apparatus as well as Dr K. Schneider and H. Scheibner for mechanical characterization measurements. This work is financed in part via the BMBF project Nanett (federal research funding of Germany FKZ: 03IS2011F).

References

- O. V. Salata, *J. Nanobiotechnol.*, 2004, **2**, 3.
- J. I. Mönch, A. Meye, A. Leonhardt, K. Krämer, R. Kozhuharova, T. Gemming, M. P. Wirth and B. Büchner, *J. Magn. Magn. Mater.*, 2005, **290-291**, 276.

- S. S. P. Parkin, *Annu. Rev. Mater. Sci.*, 1995, **25**, 257.
- M. Pannetier, C. Fermon, G. Le Goff, J. Simola and E. Kerr, *Science*, 2004, **304**, 1648.
- W. Shen, X. Liu, D. Mazumdar and G. Xiao, *Appl. Phys. Lett.*, 2005, **86**, 253901.
- Z. Jiang, J. Llandro, T. Mitrelias and J. A. C. Bland, *J. Appl. Phys.*, 2006, **99**, 08S105.
- I. Mönch, D. Makarov, R. Koseva, L. Baraban, D. Karnaushenko, C. Kaiser, K.-F. Arndt and O. G. Schmidt, *ACS Nano*, 2011, **5**, 7436.
- N. Bremond, E. Santanach-Carreras, L.-Y. Chu and J. Bibette, *Soft Matter*, 2010, **6**, 2484.
- N. Lorber, B. Pavageau and E. Mignard, *Macromolecules*, 2010, **43**, 5524.
- L. Baraban, F. Bertholle, N. Bremond, J. Baudry, P. Panizza, A. de Visser and J. Bibette, *Lab Chip*, 2011, **11**, 4057.
- M. Melzer, D. Makarov, A. Calvimontes, D. Karnaushenko, S. Baunack, R. Kaltofen, Y. F. Mei and O. G. Schmidt, *Nano Lett.*, 2011, **11**, 2522.
- R. H. Kim, D. H. Kim, J. Xiao, B. H. Kim, S. I. Park, B. Panilaitis, R. Ghaffari, J. Yao, M. Li, Z. Liu, V. Malyarchuk, D. G. Kim, A. P. Le, R. G. Nuzzo, D. L. Kaplan, F. G. Omenetto, Y. Huang, Z. Kang and J. A. Rogers, *Nat. Mater.*, 2010, **9**, 929.
- D. H. Kim, J. H. Ahn, W. M. Choi, H. S. Kim, T. H. Kim, J. Song, Y. Y. Huang, Z. Liu, C. Lu and J. A. Rogers, *Science*, 2008, **320**, 507.
- D. H. Kim, N. Lu, R. Ghaffari, Y. S. Kim, S. P. Lee, L. Xu, J. Wu, R. H. Kim, J. Song, Z. Liu, J. Viventi, B. de Graff, B. Elolampi, M. Mansour, M. J. Slepian, S. Hwang, J. D. Moss, S. M. Won, Y. Huang, B. Litt and J. A. Rogers, *Nat. Mater.*, 2011, **10**, 316.
- Y. Zhang, M. Yu, D. E. Savage, M. G. Lagally, R. H. Blick and F. Liu, *Appl. Phys. Lett.*, 2010, **96**, 11904.
- F. Cavallo and M. G. Lagally, *Soft Matter*, 2010, **6**, 439.
- N. Pamme, *Lab Chip*, 2006, **6**, 24.
- A. Fornara, P. Johansson, K. Petersson, S. Gustafsson, J. Qin, E. Olsson, D. Ilver, A. Krozer, M. Muhammed and C. Johansson, *Nano Lett.*, 2008, **8**, 3423.
- D. A. Hall, R. S. Gaster, T. Lin, S. J. Osterfeld, S. Han, B. Murmann and S. X. Wang, *Biosens. Bioelectron.*, 2010, **25**, 2051.
- D. A. Hall, R. S. Gaster, S. J. Osterfeld, B. Murmann and S. X. Wang, *Biosens. Bioelectron.*, 2010, **25**, 2177.
- C. Albon, A. Weddemann, A. Auge, D. Meissner, K. Rott, P. Jutzi and A. Hütten, *Appl. Phys. Lett.*, 2009, **95**, 163106.
- C. Albon, A. Weddemann, A. Auge, K. Rott and A. Hütten, *Appl. Phys. Lett.*, 2009, **95**, 023101.
- J. C. Rife, M. M. Miller, P. E. Sheehan, C. R. Tamanaha, M. Tondra and L. J. Whitman, *Sens. Actuators, A*, 2003, **107**, 209.
- D. J. Kubinski and H. Holloway, *J. Appl. Phys.*, 1996, **79**, 7395.
- F. Brau, H. Vandeparre, A. Sabbah, C. Poulard, A. Boudaoud and P. Damman, *Nat. Phys.*, 2011, **7**, 56.
- S. P. Lacour, S. Wagner, Z. Huang and Z. Suo, *Appl. Phys. Lett.*, 2003, **82**, 2404.